

From Prediction to Planning With Goal Conditioned Lane Graph Traversals

Marcel Hallgarten
Robert Bosch GmbH
Stuttgart, Germany
marcel.hallgarten@de.bosch.com

Martin Stoll
Robert Bosch GmbH
Stuttgart, Germany
martin.stoll@de.bosch.com

Andreas Zell
Cognitive Systems Group
University of Tübingen
Tübingen, Germany
andreas.zell@uni-tuebingen.de

Abstract—The field of motion prediction for automated driving has seen tremendous progress recently, bearing ever-more mighty neural network architectures. Leveraging these powerful models bears great potential for the closely related planning task. In this letter we propose a novel goal-conditioning method and show its potential to transform a state-of-the-art prediction model into a goal-directed planner. Our key insight is that conditioning prediction on a navigation goal at the behaviour level outperforms other widely adopted methods, with the additional benefit of increased model interpretability. We train our model on a large open-source dataset and show promising performance in a comprehensive benchmark.

Index Terms—motion prediction, behaviour planning, imitation learning, autonomous vehicles

I. INTRODUCTION

The enormous challenge of enabling autonomous driving is commonly subdivided into the tasks of perception, prediction, and planning. While perception is supposed to determine the location and type of objects and infrastructure based on raw sensor data such as RGB images or LiDAR pointclouds, prediction aims at forecasting the objects' future motion, so that a downstream planning algorithm is able to avoid collisions while navigating safely and comfortably towards a goal. Traditional approaches address these tasks separately, resulting in a tremendous engineering effort for designing, fine-tuning and adapting interfaces to new scenario types [1]. In contrast, end-to-end trainable machine learning models solve multiple tasks at once, and are thereby able to scale performance with the amount of available data. This scaling property holds especially for prediction models, where data are easy to collect and imitation learning models can be trained via supervised learning. Thus, the field of prediction has seen tremendous progress recently, fuelled by large open-source datasets and associated benchmarks [2]–[4].

However, as observation alone without knowing the intention is not sufficient to unambiguously understand and imitate an expert's decision [5], carrying over advances from prediction to planning is a challenging task. In general, passing information on a desired goal to an imitation learning model is not trivial, as the strong correlation with the learning target could mislead the learner into ignoring other important aspects, such as safety and comfort. On the other hand, goal-conditioned prediction models [6]–[8] exploit this by conditioning the prediction on several candidate targets to increase diversity.

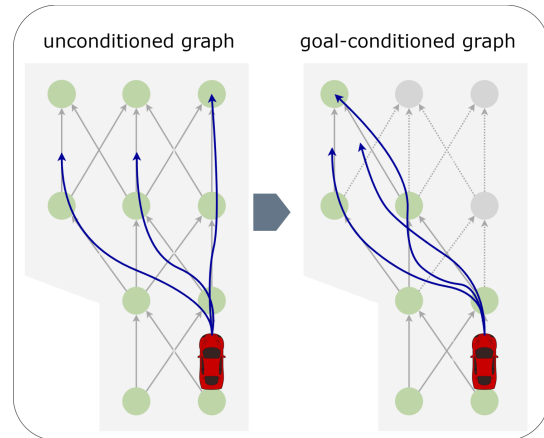


Fig. 1. Left: Candidate plans on an unconditioned graph cover all feasible behaviours, including those that do not follow the route. Right: On the conditioned graph, the model can use its entire multimodality budget to find trajectories that comply with a navigation goal, potentially yielding better plans.

In contrast, for planning blindly following a target without reasoning about safety and comfort is not desirable.

This work builds on the existing vehicle trajectory prediction model PGP [9] and introduces a novel method for goal conditioning that precludes behaviour level plans going off-route from being considered. At the same time the model retains most of its flexibility, such that it is able to circumvent the common pitfalls mentioned above. Fig. 1 illustrates the degrees of freedom before and after goal conditioning.

Recall that goal-directedness is not the only difference between prediction and planning tasks. While prediction embraces diverse trajectory forecasts, a planner must commit to a single safe, comfortable, and fast-progressing plan.

Our main contribution is as follows: We introduce a novel way to achieve goal conditioning, making it possible to carry over recent advances in the field of prediction to the planning problem. We evaluate our model in open-loop and closed-loop simulation on the nuPlan open-source dataset [10] and observe that this simple yet effective modification alone can significantly reduce the gap towards state-of-the-art planning performance. Source code will be made publicly available prior to the conference.

The remainder of this paper is structured as follows: First we discuss related work and recent advances in prediction and planning. Subsequently, in Section III we introduce a novel approach for goal-conditioned planning which is evaluated in Section IV-D. Finally, Section V draws conclusions and gives an outlook on promising future research directions.

II. RELATED WORK

Prediction and Planning for Automated Driving

The planning task aims to find a single trajectory that is optimal in terms of driving comfort, safety, efficiency, progress along route, etc. Besides rule-based approaches, which can suffer from poor generalization to new scenarios and need large engineering efforts, learning-based approaches have gained traction over recent years. Pioneering work in the 1980s [11] demonstrated lane following on public roads with a shallow dense neural network using behaviour cloning. A recent line of work combines this with optimization-based planning using cost functions learned from data [12]–[15].

The trajectory prediction task is closely related, often using similar input and output representations as for planning. Because the intentions of other traffic participants are unknown, prediction tries to cover the variety of possible future behaviours with multi-modal trajectory outputs. A large body of literature exists, with new models showing ever-increased performance on public benchmarks [16]–[22].

Despite their similarities, prediction and planning are often tackled as separate, sequential tasks [23], [24], or in a joint end-to-end fashion [14], [15] (see [1] for a comprehensive survey). [25] explicitly couples the self-driving vehicle’s (SDV) future plan with other traffic participants’ predictions, enabling mutually contingent planning. In this work we exploit the similarity of the prediction and planning tasks by leveraging an existing state-of-the-art prediction model for goal-directed trajectory planning.

From Grids to Graphs

Representing the environment in the form of rasterized grids in combination with convolutional neural network architectures has been a very popular approach for trajectory prediction [26]–[30]. In recent years a new generation of models emerged, that relies on graph neural networks or attention blocks to model interactions [19], [31]–[36]. Similarly, recent models achieve increased performance by exploiting graph based representations for the map [9], [17], [18], [31], [37]. We refer the reader to [38] for a comprehensive survey. This innovation has not yet completely carried over to the planning task, with [8], [39] being notable exceptions.

Goal Conditioning

A key challenge to repurpose a prediction model for planning is how to condition the diverse, multi-modal outputs on a given intention, i.e. the navigation goal. The two predominant alternatives are to either switch between specialized submodels depending on a high-level command, or add additional model inputs [5]. The former is an effective way to reduce imbalance

in the training set and has been successfully applied in [15]. However, as the number of high-level commands and their definition have to be fixed in advance, this comes at the cost of flexibility. The latter approach, which inputs the intention to the model directly, has been applied more broadly [40]–[44]. As already observed in [5] these models are only implicitly conditioned on the intention, with the risk that the route is not always followed. Our approach circumvents this risk by conditioning directly on road graph level.

Another way to encourage goal-directed planning is the addition of a cost term that favours progress on route [14]. The optimizer then has to find a balance between progress and other objectives such as safety and comfort, possibly sacrificing one for the other.

Goal-Conditioning Prediction as Planning

Two-step prediction approaches first identify a set of targets, and then employ a decoder that regresses a trajectory to each target. [8] decodes trajectories conditioned on a target lane, whereas [6], [7] use the same paradigm but condition on concrete spatial locations or sparsely sampled trajectories [16]. Most similar to our work is [9], which conditions predictions on a coarse path represented by a traversal of the lane graph, whereby this path does not include any temporal information, such as the velocity profile nor exact spatial locations. Since their approach primarily seeks to increase diversity through traversals and learns the corresponding probabilities purely from imitation, routing is not considered. We show that this opens up an opportunity to define a new method of target conditioning directly on the lane graph traversal, since the SDV is still able and required to reason about safety in order to infer a velocity profile and plan the exact trajectory.

III. MODEL DESCRIPTION

A. Graph-Based Prediction Model

We give a brief recap of PGP [9], upon which our model is based.

1) *Encoder*: The encoder builds a graph representation of the environment centred around a road graph $G(V, E)$.

Lane centrelines are divided into snippets of similar length and discretized into a polyline with fixed maximum length. Binary flags for stop lines and crosswalks are added to the poses. The lane centreline snippets form the graph nodes V . Directed edges E indicate allowed transitions between nodes: E_{succ} for successor nodes along the lane in the direction of traffic flow and E_{prox} for proximal nodes on neighbouring lanes.

For each agent i in the scene its history is represented as a trajectory $s^i = [x_t^i, y_t^i, v_t^i, a_t^i, \omega_t^i, I^i]_{t=-t_h}^0$, where x_t^i, y_t^i are the position at timestep t within the observation horizon t_h given in the SDV’s local cartesian coordinate frame, v_t^i, a_t^i, ω_t^i are speed, acceleration, and yaw rate, respectively. I^i is an indicator for object type (vehicle or pedestrian).

Polylines, agent history, and SDV history are all encoded using gated recurrent units (GRU), yielding encodings h_{node} , h_{agent}^i , and h_{SDV} . Agent-to-node attention allows the lane nodes

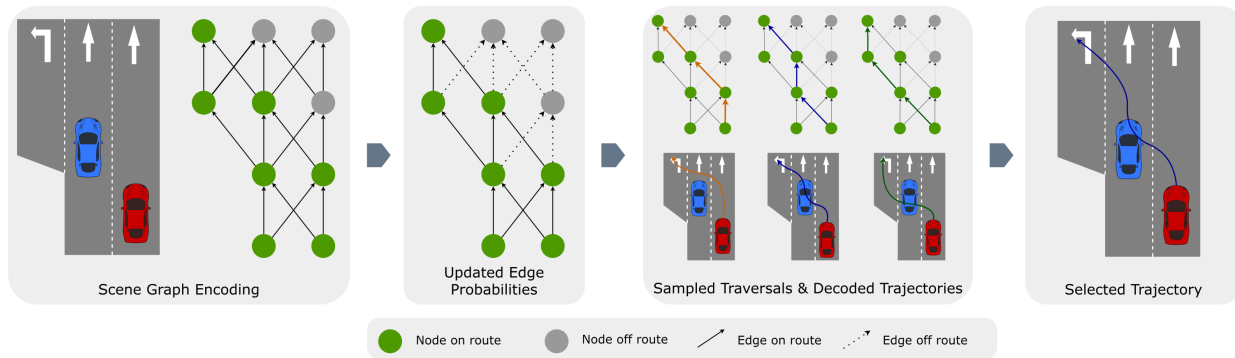


Fig. 2. Model overview: We manipulate the edge probabilities of a graph-based scene representation to decode route-conditioned candidate plans and select a goal-directed trajectory for the SDV.

to accumulate traffic information, before graph neural network (GNN) layers are applied to the road graph. The full encoding is given by $h_{\text{agg}}^v \forall v \in V$.

2) *Graph Traversals*: The "aggregator" module determines transition probabilities for all edges and samples traversals through the graph.

For each node $u \in V$, the probabilities of all outgoing edges (u, v) are determined from regressed edge scores,

$$\pi(u, v) = \text{softmax}(\text{score}(u, v) \mid (u, v) \in E). \quad (1)$$

Graph traversals are obtained from an initial node via sampling from these edge probabilities. In order to allow traversals of arbitrary length (up to a maximum number of nodes T), terminal edges are added to each node. At inference time, K traversals $\{v_n^{(k)}\}_{n=0}^T, k = 1, \dots, K$ are sampled.

3) *Trajectory Decoder*: From a given traversal

$$h_{\text{traversal}}^k = \phi(h_{\text{agg}}^v \forall v \in \{v_n^k\}_{n=0}^T), \quad (2)$$

a latent variable model decodes the predicted trajectory

$$o^k = \text{MLP}(\phi(h_{\text{traversal}}^k, h_{\text{SDV}}, z)). \quad (3)$$

ϕ denotes concatenation and z is a random noise vector to enhance variety. In practise a large number of traversals is sampled and a fixed number of output trajectories is obtained after k -means clustering.

B. Route-Conditioned Traversals

Our goal is to ensure goal conditioning of the trajectory output at the behaviour level. To this end we manipulate the edge probabilities obtained by the prediction model in a way that makes traversals that follow the intended route more likely. An overview of our method is depicted in Fig. 2. All nodes that lie on a path between the SDV's current position and the navigation goal are considered "on route", and the corresponding edges form the set E_{route} .

We propose two methods for conditioning road-graph traversals. Firstly, we enhance edge probabilities that stay on route with an additive bonus

$$\pi(u, v) = \text{softmax}(\text{score}(u, v) + \beta \cdot \mathbb{1}_{(u, v) \in E_{\text{route}}} \mid (u, v) \in E), \quad (4)$$

where $\mathbb{1}_{(u, v) \in E_{\text{route}}}$ indicates whether the edge (u, v) lies on-route. The magnitude of the bonus β is identical for all edges and is a learnable model parameter. We call this setup *soft-mask* goal conditioning.

Alternatively, we apply a *hard mask* by setting the probabilities of edges that do not follow the route to zero. This provides a guarantee that all traversals comply with the navigation goal. The updated probabilities are given by

$$\pi(u, v) = \text{softmax}(\text{score}(u, v) \mid (u, v) \in E_{\text{route}}). \quad (5)$$

We can apply the hard mask at inference time only (subsequently referred to as *Goal-Conditioned PGP (GC-PGP)*), or already during training (termed *hard mask*). Applying the mask only at inference time is also beneficial from a theoretical viewpoint, because the model still learns the entire multi-modal distribution, and no re-training is necessary.

C. Trajectory Selection

For a prediction model it is a natural choice to output multiple trajectories per agent in order to account for the multi-modality induced by uncertain intention. In contrast, for the planning task the model has to commit to a single trajectory. Similar to [45] we apply a simple heuristic and select the trajectory with highest probability.

Note that this choice does not necessarily correspond to the predominant road graph traversal (due to the clustering step).

IV. EXPERIMENTS

A. Dataset and Evaluation Framework

We employ the nuPlan dataset and framework [10] for model training and evaluation. The dataset includes diverse scenarios, e.g. making turns, yielding to pedestrians, stopping at intersections, traversing intersections and driving at different speeds. The full nuPlan train split consists of more than 30 million scenarios totalling over 1,300 hours of real-world driving. For training we use a balanced subset by restricting each scenario type to a maximum of 4,000 scenarios, resulting in approx. 150,000 scenarios. The nuPlan test split consists of 4,539 scenarios. We noticed annotation errors in some of these samples, which results in relevant lanes being labelled as off-route and vice versa. Since this is a particularly harmful in

the context of target conditioning, we remove these samples from the test set. By sampling a maximum of 30 scenarios for each available scenario type and removing the ones that are compromised by labelling errors, we obtain a test set consisting of 1,363 diverse driving scenarios. In addition we report results on a subset that focuses on scenarios where knowing the navigation goal is crucial. We limit this reduced test set to the following four scenario types at 100 scenarios each: traversing intersection, starting unprotected noncross turn, starting protected cross turn, and starting right turn. After removing the compromised samples, this intersection test split consists of 323 scenarios.

B. Metrics

Besides the aggregated driving score defined by the nuPlan framework, we also report average displacement error (ADE), final displacement error (FDE), and miss rate (MR) for the open-loop evaluations. MR is defined by the final waypoint of the 8 second planning horizon deviating more than 16 metres from ground truth. For the closed-loop simulations, we evaluate progress, driveable area compliance, and collision avoidance. Progress is given by the fraction of the travelled distance along the ground truth path. Driveable area compliance describes the share of frames where the SDV’s entire bounding box is on the driveable surface. In order to evaluate collision avoidance, we report the fraction of successful scenarios in terms of at-fault collisions. The SDV is considered to be at fault for a collision if it collides with a stationary agent or if the collision occurs at its front or sides. We train and evaluate each model twice, and report mean and standard deviation for all metrics.

C. Baselines and Ablations

Intelligent Driver Model + MOBIL baseline: IDM [46] is a simple heuristic model that can keep a safe distance to the vehicle ahead. Its extension MOBIL [47] also handles lane changes. We use the implementation provided by the nuPlan framework [10].

Urban Driver baseline: We compare our model to a state-of-the-art planning approach, which has been made available together with the nuPlan framework. Urban Driver [39] uses PointNet layers to encode the SDV’s motion as well as observed agents’ history and map elements. Subsequently, the information is fused using multi-head attention. Then a trajectory for the SDV is decoded from the aggregated encoding. In contrast to our method, for this baseline the route information is encoded into the map features. The model is fairly large (2.2M parameters), so we adapt its complexity for improved comparability to PGP (150k parameters). We reduce the encoding size from 256 to 128 and the number of subgraph layers from 3 to 2, resulting in 520k parameters (*UD-520k*). Similarly, the *UD-150k* model uses an encoding size of 64, but retains all 3 subgraph layers, totalling 150k parameters.

Filter on route baseline: The multi-modal output of PGP is post-conditioned on the route: To this end, we only keep trajectories whose end point is within 5 metres to the nearest

lane centre on route; among those we pick the trajectory with the largest probability. If no trajectory is within the distance threshold, we pick the one closest to the route.

Node features: An alternative to explicitly conditioning a model on the navigation goal is to extend the model’s input features [11]. We add a single boolean value to the lane graph’s node features that indicates whether or not the node is part of the route. This way the aggregator is conditioned directly on the route.

Soft mask: The transition probabilities of edges that keep the traversal on route receive a (learnable) bonus, see eq. (4).

Hard mask: As opposed to our GC-PGP model, edges that leave the route are removed, also at train time (see eq. (5)). This way both the aggregator and trajectory decoder models are restricted to only goal-reaching traversals.

D. Open-Loop Simulation

TABLE I
OPEN-LOOP EVALUATION ON THE ENTIRE TEST SPLIT

Model	Score	ADE [m]	FDE [m]	MR
IDM/MOBIL	0.33	7.98	12.8	0.42
Urban Driver	0.84 ± 0.01	1.42 ± 0.00	2.99 ± 0.07	0.06 ± 0.00
UD-520k	0.83 ± 0.00	1.49 ± 0.03	3.18 ± 0.08	0.06 ± 0.02
UD-150k	0.80 ± 0.01	1.62 ± 0.02	3.39 ± 0.00	0.08 ± 0.00
PGP	0.69 ± 0.02	1.82 ± 0.06	4.21 ± 0.14	0.14 ± 0.00
GC-PGP (ours)	0.76 ± 0.01	1.59 ± 0.03	3.65 ± 0.09	0.12 ± 0.01
Filter on route	0.73 ± 0.01	1.66 ± 0.01	3.84 ± 0.03	0.13 ± 0.00
Node features	0.73 ± 0.01	1.70 ± 0.02	3.91 ± 0.02	0.13 ± 0.00
Soft mask	0.71 ± 0.00	1.75 ± 0.00	4.02 ± 0.05	0.14 ± 0.01
Hard mask	0.62 ± 0.04	2.23 ± 0.27	4.82 ± 0.99	0.17 ± 0.05

TABLE II
OPEN-LOOP EVALUATION ON INTERSECTION SCENARIOS

Model	Score	ADE [m]	FDE [m]	MR
IDM/MOBIL	0.19	4.89	5.81	0.20
Urban Driver	0.83 ± 0.00	1.66 ± 0.02	3.36 ± 0.03	0.05 ± 0.00
UD-520k	0.81 ± 0.00	1.80 ± 0.04	3.73 ± 0.09	0.07 ± 0.00
UD-150k	0.77 ± 0.00	1.96 ± 0.04	4.03 ± 0.08	0.08 ± 0.00
PGP	0.56 ± 0.03	2.48 ± 0.08	5.67 ± 0.20	0.19 ± 0.01
GC-PGP (ours)	0.74 ± 0.01	1.80 ± 0.04	4.03 ± 0.11	0.10 ± 0.00
Filter on route	0.68 ± 0.01	1.98 ± 0.01	4.50 ± 0.04	0.14 ± 0.00
Node features	0.67 ± 0.02	2.15 ± 0.07	4.81 ± 0.12	0.14 ± 0.01
Soft mask	0.60 ± 0.00	2.41 ± 0.00	5.43 ± 0.05	0.19 ± 0.01
Hard mask	0.67 ± 0.04	2.20 ± 0.15	4.92 ± 0.29	0.16 ± 0.03

We report in Tab. I open-loop imitation performance on the full, diverse test split. This dataset is dominated by scenarios where route information is not required, such as being stationary at traffic lights or simple lane following. We observe that all goal-conditioning variants still out-perform the (undirected) PGP baseline in all metrics, closely approaching the strong Urban Driver baseline. Interestingly enough the IDM/MOBIL model is a poor contestant w.r.t. imitation metrics: its behaviour may have desirable properties, but it is not particularly human-like on nuPlan scenarios.

To demonstrate the effectiveness of our approach we also evaluate on a reduced test set as described in Sec. IV-A. This dataset is focused on non-trivial intersection scenarios where

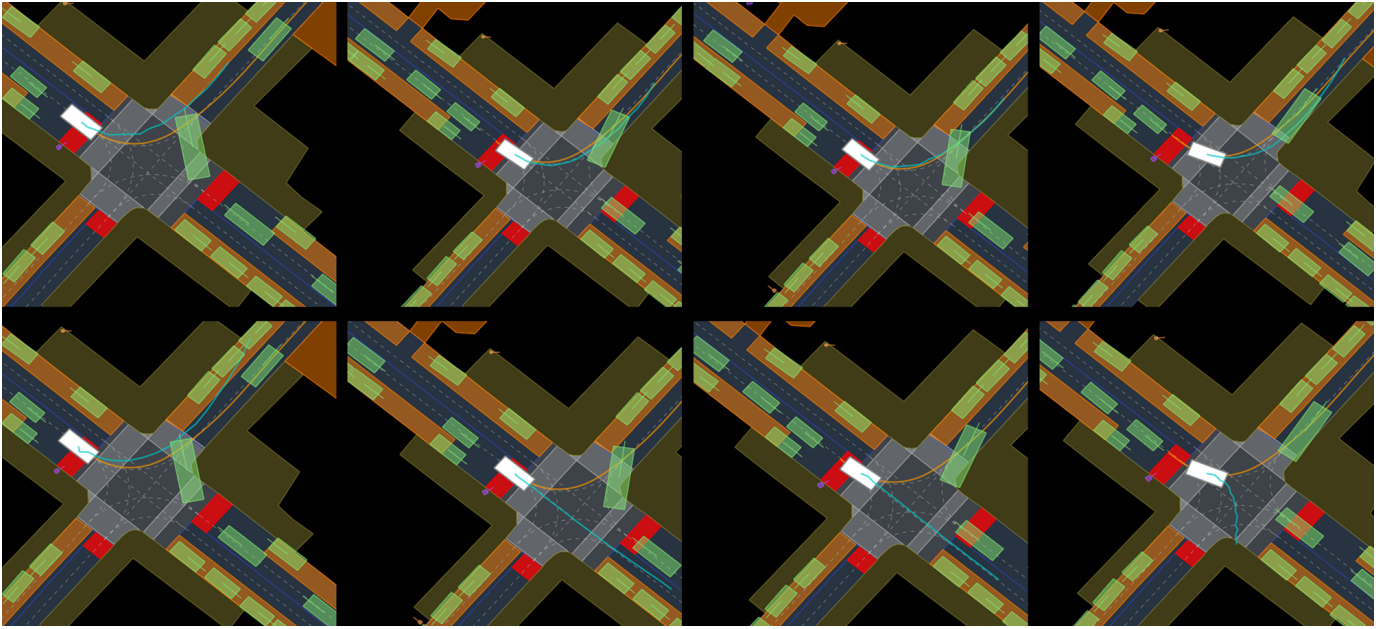


Fig. 3. Qualitative results: Left to right depicts the the first 4 seconds of the SDV making a left turn. Top: GC-PGP, Bottom: *node features* ablation. The expert trajectory and model prediction are depicted in orange and blue respectively. The orange surface indicates parking areas. Stoplines are shown in red. In the bottom row toggling between turning and going straight manoeuvres can be observed, whereas our model (top) is compliant with the route at all times. (Best viewed in colour.)

the navigation goal is important to the driving behaviour. Results are reported in Tab. II and confirm our previous observations. Our goal-conditioned model (GC-PGP) clearly outperforms the PGP prediction baseline and catches up to the Urban Driver planner baseline in overall score and displacement error.

Looking at alternative goal-conditioning methods we observe that the *node features* and *soft mask* models only show mild improvements over PGP. We speculate that they do not always strictly adhere to the route information, a claim that is supported by qualitative results in Fig. 3. In contrast, the masking in our GC-PGP model prevents taking plans off the route into consideration. However, we note that applying this hard mask also at train time to focus on goal-directed traversals only compromises performance. This model is much less robust against route labelling errors as described in Sec. IV-A and we hypothesize about a connection between the resulting faulty mask and observed instabilities during training.

E. Temporal Plan Stability

TABLE III
TEMPORAL PLAN INSTABILITY ON INTERSECTION SCENARIOS

Model	TPI [m]
IDM/MOBIL	0.58
Urban Driver	1.51 ± 0.00
UD-520k	1.78 ± 0.02
UD-150k	1.84 ± 0.14
PGP	3.65 ± 0.15
GC-PGP (ours)	2.80 ± 0.00

The deviation between planned trajectories for consecutive timesteps is a measure for robustness of the planner. A low value means that the plans are consistent over time, indicating robustness and resulting in a comfortable driving experience. We define temporal plan instability (TPI)

$$\text{tpi}(\tau) = \|(x, y)_{T}^{\textcircled{\tau}} - (x, y)_{T-1}^{\textcircled{\tau+1}}\|_2 \quad (6)$$

the distance between (adjusted) trajectory end-points for consecutive timesteps ($\textcircled{\tau}$, $\textcircled{\tau+1}$) and report results in Tab. III.

The IDM/MOBIL baseline produces the most time-consistent plans and can serve as a lower limit, which is unsurprising given its underlying simple heuristics. PGP is the least time-consistent model. As a prediction model, it has been designed to produce diverse trajectories, both w.r.t. the route taken, and different velocity profiles. Toggling between these modes naturally leads to large plan instability. Conditioning on a navigation goal (GC-PGP) removes the main source of multimodality, but diversity w.r.t. velocity remains as a cause for instability. GC-PGP thus yields more stable plans compared to PGP, but retains a higher degree of toggling than Urban Driver, an inherently unimodal planning model. This indicates that the naïve way we select a trajectory among the multimodal proposals may not be ideal. Consequently, planning performance could be further improved by applying a cost function that balances different aspects of driving, such as safety, comfort, progress, etc., as in [14], [15].

F. Closed-Loop Simulation

We also evaluate all models in the log-playback closed-loop simulation environment provided by the nuPlan framework. The same reduced test set as for the open-loop evaluation is

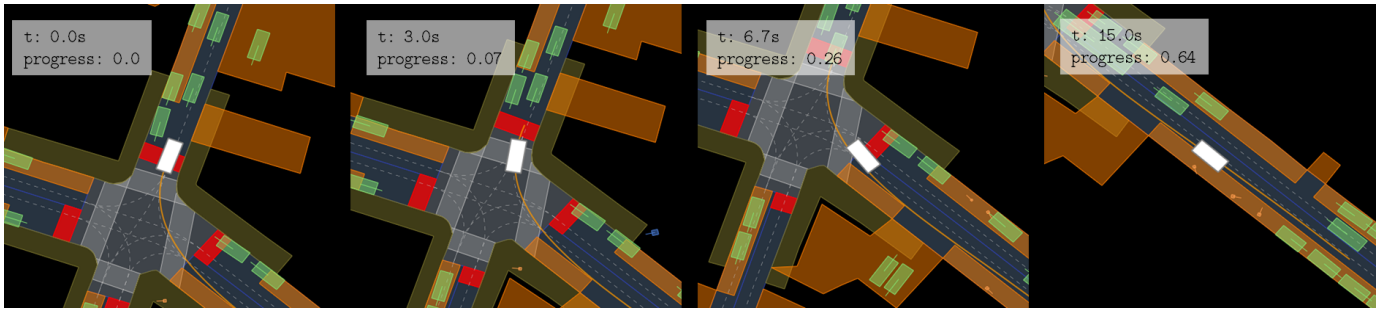


Fig. 4. Making a turn in closed-loop simulation. The SDV enters the intersection after 3 seconds having travelled 7% of the expert’s total travelled distance and leaves the intersection after 6.7 seconds with 26% progress. In total it covers 64% of the expert’s path during the 15 seconds of simulation. (Best viewed in colour.)

TABLE IV
CLOSED-LOOP EVALUATION ON INTERSECTION SCENARIOS

Model	Score	Progress	Driv. Area	Col.-Free
IDM/MOBIL	0.75	0.81	0.96	0.90
Urban Driver	0.58 ± 0.06	0.76 ± 0.11	0.89 ± 0.02	0.85 ± 0.01
UD-520k	0.50 ± 0.08	0.71 ± 0.06	0.90 ± 0.02	0.84 ± 0.02
UD-150k	0.45 ± 0.02	0.74 ± 0.08	0.81 ± 0.01	0.79 ± 0.03
PGP	0.37 ± 0.05	0.36 ± 0.07	0.88 ± 0.04	0.89 ± 0.03
GC-PGP (ours)	0.46 ± 0.03	0.47 ± 0.08	0.88 ± 0.01	0.88 ± 0.04
Filter on route	0.43 ± 0.02	0.43 ± 0.09	0.87 ± 0.04	0.87 ± 0.01
Node features	0.37 ± 0.00	0.37 ± 0.03	0.86 ± 0.05	0.87 ± 0.03
Soft mask	0.29 ± 0.02	0.30 ± 0.06	0.91 ± 0.00	0.92 ± 0.02
Hard mask	0.43 ± 0.04	0.43 ± 0.06	0.84 ± 0.01	0.84 ± 0.01

used (cf. Sec. IV-A). Results are presented in Tab. IV. It is striking that the hand-crafted IDM/MOBIL model achieves the best overall performance by a large margin, but is still not perfectly safe in terms of drivable area compliance and caused collisions. This completes the picture we gained from open-loop evaluation (Sec. IV-D): IDM/MOBIL is a fairly strong “classical” baseline, just not in terms of expert imitation.

Both PGP and GC-PGP are on par with Urban Driver regarding drivable area compliance, and even outperform w.r.t. caused collisions. Although GC-PGP improves upon (the undirected) PGP in terms of progress along the route, with a value of 0.47 it still falls behind Urban Driver. See Fig. 4 to put this value into perspective: At some point well behind the crossing, GC-PGP fails to progress along the lane fast enough. We conclude that an average progress of only 0.47 is on average sufficient to master the crossing, but indicates shortcomings in the subsequent lane following task, which exceeds the scope of our method.

For the alternative goal-conditioning approaches (lower part of Tab. IV), we do not observe significant deviations from their PGP and GC-PGP counterparts w.r.t. drivable area compliance and caused collisions. Instead we do find that they all achieve less progress than GC-PGP, the *soft mask* variant being even worse than the PGP baseline. These results confirm GC-PGP as the most performant variant to condition PGP on a navigation goal.

V. CONCLUSIONS

In this work, we presented a novel way to achieve goal conditioning on a graph-based map representation that precludes behaviour level plans going off-route from being considered. We demonstrated the effectiveness of our approach in a comprehensive benchmark against rule-based and data-based models. Most importantly, we observe that goal conditioning at the behaviour level is able to substantially improve goal-directed driving without compromising further important aspects, such as safety and comfort.

Our method facilitates repurposing of state-of-the-art prediction models for the planning task. We experimentally confirmed that inducing goal-directedness is an essential aspect of this quest. In order to enable a smooth and comfortable driving experience, a planner also needs to consistently select from multi-modal trajectory candidates. We will address this uni-modality problem in future work.

Additionally, we plan to extend the proposed approach by restricting traversals to incorporate further rule-based aspects of planning, such as stopping before red lights.

REFERENCES

- [1] A. Tampuu, T. Matiisen, M. Semikin, D. Fishman, and N. Muhammad, “A survey of end-to-end driving: Architectures and training methods,” *IEEE Transactions on Neural Networks and Learning Systems*, 2020.
- [2] S. Ettinger, S. Cheng, B. Caine, C. Liu, H. Zhao, S. Pradhan, Y. Chai, B. Sapp, C. R. Qi, Y. Zhou *et al.*, “Large scale interactive motion forecasting for autonomous driving: The waymo open motion dataset,” in *Proceedings of the IEEE/CVF International Conference on Computer Vision*, 2021, pp. 9710–9719.
- [3] H. Caesar, V. Bankiti, A. H. Lang, S. Vora, V. E. Liong, Q. Xu, A. Krishnan, Y. Pan, G. Baldan, and O. Beijbom, “nusenes: A multimodal dataset for autonomous driving,” in *Proceedings of the IEEE/CVF conference on computer vision and pattern recognition*, 2020, pp. 11 621–11 631.
- [4] B. Wilson, W. Qi, T. Agarwal, J. Lambert, J. Singh, S. Khandelwal, B. Pan, R. Kumar, A. Hartnett, J. K. Pontes *et al.*, “Argoverse 2: Next generation datasets for self-driving perception and forecasting,” *arXiv preprint arXiv:2301.00493*, 2023.
- [5] F. Codevilla, M. Müller, A. López, V. Koltun, and A. Dosovitskiy, “End-to-end driving via conditional imitation learning,” in *2018 IEEE international conference on robotics and automation (ICRA)*. IEEE, 2018, pp. 4693–4700.
- [6] H. Zhao, J. Gao, T. Lan, C. Sun, B. Sapp, B. Varadarajan, Y. Shen, Y. Shen, Y. Chai, C. Schmid *et al.*, “Tnt: Target-driven trajectory prediction,” in *Conference on Robot Learning*. PMLR, 2021, pp. 895–904.

- [7] J. Gu, C. Sun, and H. Zhao, "Densetnet: End-to-end trajectory prediction from dense goal sets," in *Proceedings of the IEEE/CVF International Conference on Computer Vision*, 2021, pp. 15 303–15 312.
- [8] J. Wang, T. Ye, Z. Gu, and J. Chen, "Ltp: Lane-based trajectory prediction for autonomous driving," in *Proceedings of the IEEE/CVF Conference on Computer Vision and Pattern Recognition*, 2022, pp. 17 134–17 142.
- [9] N. Deo, E. Wolff, and O. Beijbom, "Multimodal trajectory prediction conditioned on lane-graph traversals," in *Conference on Robot Learning*. PMLR, 2022, pp. 203–212.
- [10] H. Caesar, J. Kabzan, K. S. Tan, W. K. Fong, E. Wolff, A. Lang, L. Fletcher, O. Beijbom, and S. Omari, "nuPlan: A closed-loop ml-based planning benchmark for autonomous vehicles," *arXiv preprint arXiv:2106.11810*, 2021.
- [11] D. A. Pomerleau, "Alvin: An autonomous land vehicle in a neural network," *Advances in neural information processing systems*, vol. 1, 1988.
- [12] W. Zeng, W. Luo, S. Suo, A. Sadat, B. Yang, S. Casas, and R. Urtasun, "End-to-end interpretable neural motion planner," in *Proceedings of the IEEE/CVF Conference on Computer Vision and Pattern Recognition*, 2019, pp. 8660–8669.
- [13] B. Wei, M. Ren, W. Zeng, M. Liang, B. Yang, and R. Urtasun, "Perceive, attend, and drive: Learning spatial attention for safe self-driving," in *2021 IEEE International Conference on Robotics and Automation (ICRA)*. IEEE, 2021, pp. 4875–4881.
- [14] A. Sadat, S. Casas, M. Ren, X. Wu, P. Dhawan, and R. Urtasun, "Perceive, predict, and plan: Safe motion planning through interpretable semantic representations," in *European Conference on Computer Vision*. Springer, 2020, pp. 414–430.
- [15] S. Casas, A. Sadat, and R. Urtasun, "Mp3: A unified model to map, perceive, predict and plan," in *Proceedings of the IEEE/CVF Conference on Computer Vision and Pattern Recognition*, 2021, pp. 14 403–14 412.
- [16] Q. Lu, W. Han, J. Ling, M. Wang, H. Chen, B. Varadarajan, and P. Covington, "Kemp: Keyframe-based hierarchical end-to-end deep model for long-term trajectory prediction," *arXiv preprint arXiv:2205.04624*, 2022.
- [17] B. Varadarajan, A. Hefny, A. Srivastava, K. S. Refaat, N. Nayakanti, A. Cornman, K. Chen, B. Douillard, C. P. Lam, D. Anguelov *et al.*, "Multipath++: Efficient information fusion and trajectory aggregation for behavior prediction," in *2022 International Conference on Robotics and Automation (ICRA)*. IEEE, 2022, pp. 7814–7821.
- [18] M. Liang, B. Yang, R. Hu, Y. Chen, R. Liao, S. Feng, and R. Urtasun, "Learning lane graph representations for motion forecasting," in *European Conference on Computer Vision*. Springer, 2020, pp. 541–556.
- [19] N. Nayakanti, R. Al-Rfou, A. Zhou, K. Goel, K. S. Refaat, and B. Sapp, "Wayformer: Motion forecasting via simple & efficient attention networks," *arXiv preprint arXiv:2207.05844*, 2022.
- [20] M. Ye, J. Xu, X. Xu, T. Cao, and Q. Chen, "Dcms: Motion forecasting with dual consistency and multi-pseudo-target supervision," *arXiv preprint arXiv:2204.05859*, 2022.
- [21] M. Ye, T. Cao, and Q. Chen, "Tpcn: Temporal point cloud networks for motion forecasting," in *Proceedings of the IEEE/CVF Conference on Computer Vision and Pattern Recognition*, 2021, pp. 11 318–11 327.
- [22] S. Shi, L. Jiang, D. Dai, and B. Schiele, "Mtr-a: 1st place solution for 2022 waymo open dataset challenge–motion prediction," *arXiv preprint arXiv:2209.10033*, 2022.
- [23] S. Thrun, M. Montemerlo, H. Dahlkamp, D. Stavens, A. Aron, J. Diebel, P. Fong, J. Gale, M. Halpenny, G. Hoffmann *et al.*, "Stanley: The robot that won the darpa grand challenge," *Journal of field Robotics*, vol. 23, no. 9, pp. 661–692, 2006.
- [24] M. Montemerlo, J. Becker, S. Bhat, H. Dahlkamp, D. Dolgov, S. Ettinger, D. Haehnel, T. Hilden, G. Hoffmann, B. Huhnke *et al.*, "Junior: The stanford entry in the urban challenge," *Journal of field Robotics*, vol. 25, no. 9, pp. 569–597, 2008.
- [25] N. Rhinehart, J. He, C. Packer, M. A. Wright, R. McAllister, J. E. Gonzalez, and S. Levine, "Contingencies from observations: Tractable contingency planning with learned behavior models," *arXiv preprint arXiv:2104.10558*, 2021.
- [26] H. Cui, V. Radosavljevic, F.-C. Chou, T.-H. Lin, T. Nguyen, T.-K. Huang, J. Schneider, and N. Djuric, "Multimodal trajectory predictions for autonomous driving using deep convolutional networks," in *2019 International Conference on Robotics and Automation (ICRA)*. IEEE, 2019, pp. 2090–2096.
- [27] T. Gilles, S. Sabatini, D. Tsishkou, B. Stanculescu, and F. Moutarde, "Home: Heatmap output for future motion estimation," in *2021 IEEE International Intelligent Transportation Systems Conference (ITSC)*. IEEE, 2021, pp. 500–507.
- [28] W. Luo, B. Yang, and R. Urtasun, "Fast and furious: Real time end-to-end 3d detection, tracking and motion forecasting with a single convolutional net," in *Proceedings of the IEEE conference on Computer Vision and Pattern Recognition*, 2018, pp. 3569–3577.
- [29] Y. Chai, B. Sapp, M. Bansal, and D. Anguelov, "Multipath: Multiple probabilistic anchor trajectory hypotheses for behavior prediction," *arXiv preprint arXiv:1910.05449*, 2019.
- [30] T. Phan-Minh, E. C. Grigore, F. A. Boulton, O. Beijbom, and E. M. Wolff, "Covnet: Multimodal behavior prediction using trajectory sets," in *Proceedings of the IEEE/CVF Conference on Computer Vision and Pattern Recognition*, 2020, pp. 14 074–14 083.
- [31] T. Gilles, S. Sabatini, D. Tsishkou, B. Stanculescu, and F. Moutarde, "Thomas: Trajectory heatmap output with learned multi-agent sampling," *arXiv preprint arXiv:2110.06607*, 2021.
- [32] Y. Yuan, X. Weng, Y. Ou, and K. M. Kitani, "Agentformer: Agent-aware transformers for socio-temporal multi-agent forecasting," in *Proceedings of the IEEE/CVF International Conference on Computer Vision*, 2021, pp. 9813–9823.
- [33] S. Khandelwal, W. Qi, J. Singh, A. Hartnett, and D. Ramanan, "What-if motion prediction for autonomous driving," *arXiv preprint arXiv:2008.10587*, 2020.
- [34] S. Casas, C. Gulino, R. Liao, and R. Urtasun, "Spagnn: Spatially-aware graph neural networks for relational behavior forecasting from sensor data," in *2020 IEEE International Conference on Robotics and Automation (ICRA)*. IEEE, 2020, pp. 9491–9497.
- [35] J. Gao, C. Sun, H. Zhao, Y. Shen, D. Anguelov, C. Li, and C. Schmid, "Vectornet: Encoding hd maps and agent dynamics from vectorized representation," in *Proceedings of the IEEE/CVF Conference on Computer Vision and Pattern Recognition*, 2020, pp. 11 525–11 533.
- [36] A. Knittel, M. Hawasly, S. V. Albrecht, J. Redford, and S. Ramamoorthy, "Dipa: Diverse and probabilistically accurate interactive prediction," *arXiv preprint arXiv:2210.06106*, 2022.
- [37] T. Gilles, S. Sabatini, D. Tsishkou, B. Stanculescu, and F. Moutarde, "Gohome: Graph-oriented heatmap output for future motion estimation," in *2022 International Conference on Robotics and Automation (ICRA)*. IEEE, 2022, pp. 9107–9114.
- [38] J. Liu, X. Mao, Y. Fang, D. Zhu, and M. Q.-H. Meng, "A survey on deep-learning approaches for vehicle trajectory prediction in autonomous driving," in *2021 IEEE International Conference on Robotics and Biomimetics (ROBIO)*. IEEE, 2021, pp. 978–985.
- [39] O. Scheel, L. Bergamini, M. Wolczyk, B. Osiński, and P. Ondruska, "Urban driver: Learning to drive from real-world demonstrations using policy gradients," in *Conference on Robot Learning*. PMLR, 2022, pp. 718–728.
- [40] K. Chitta, A. Prakash, and A. Geiger, "Neat: Neural attention fields for end-to-end autonomous driving," in *Proceedings of the IEEE/CVF International Conference on Computer Vision*, 2021, pp. 15 793–15 803.
- [41] A. Prakash, K. Chitta, and A. Geiger, "Multi-modal fusion transformer for end-to-end autonomous driving," in *Conference on Computer Vision and Pattern Recognition (CVPR)*, 2021.
- [42] H. Shao, L. Wang, R. Chen, H. Li, and Y. Liu, "Safety-enhanced autonomous driving using interpretable sensor fusion transformer," *arXiv preprint arXiv:2207.14024*, 2022.
- [43] P. Wu, X. Jia, L. Chen, J. Yan, H. Li, and Y. Qiao, "Trajectory-guided control prediction for end-to-end autonomous driving: A simple yet strong baseline," *arXiv preprint arXiv:2206.08129*, 2022.
- [44] D. Chen and P. Krähenbühl, "Learning from all vehicles," in *Proceedings of the IEEE/CVF Conference on Computer Vision and Pattern Recognition*, 2022, pp. 17 222–17 231.
- [45] S. Pini, C. S. Perone, A. Ahuja, A. S. R. Ferreira, M. Niendorf, and S. Zagoruyko, "Safe real-world autonomous driving by learning to predict and plan with a mixture of experts," *arXiv preprint arXiv:2211.02131*, 2022.
- [46] M. Treiber, A. Hennecke, and D. Helbing, "Congested traffic states in empirical observations and microscopic simulations," *Physical review E*, vol. 62, no. 2, p. 1805, 2000.
- [47] A. Kesting, M. Treiber, and D. Helbing, "General lane-changing model mobil for car-following models," *Transportation Research Record*, vol. 1999, no. 1, pp. 86–94, 2007.